https://doi.org/10.3311/PPci.21360

Periodica Polytechnica Civil Engineering, 67(1), pp. 261–271, 2023

A Parametric Investigation of the Influence of Knots on the Flexural Behavior of Timber Beams

Khaled Saad[1], András Lengyel[1*]

[1] Department of Structural Mechanics, Budapest University of Technology and Economics, H-1521 Budapest, P.O.B. 91, Hungary
[*] Corresponding author, e-mail: lengyel.andras@emk.bme.hu

Received: 17 October 2022, Accepted: 17 November 2022, Published online: 01 December 2022

Abstract

The presence of knots significantly influences the mechanical behavior of timber. This research presents a parametric finite element analysis of the effect of knot characteristics on the flexural capacity of timber beams. Parameters include knot radius, longitudinal and vertical positions, length, and diving angle. The generation of the FE model is based on a technique developed in a previous research stage. The validation of the model is done via bending tests on a set of beams as well as a number of independent research studies. The numerical model accurately recreates the three-dimensional geometry of the knot and related fiber deviations. The capacity of the beams under bending is evaluated via the Tsai–Wu failure criterion. Findings reveal that the presence of knots in the tension zone leads to an early tensile failure and insufficient utilization of compression capacity, the decrease of bending capacity may rise significantly (up to 39% in this investigation), the knot inclination may positively or negatively influence the behavior depending on the diving angle, and moderate knot length can be detrimental to flexural capacity.

Keywords

knot, timber, fiber deviation, parametric finite element modelling, Norway spruce

1 Introduction

Wood has played a significant role in construction throughout human history as one of the most fundamental building materials. Despite the advancement of artificial materials such as steel and concrete in our modern age, wood has preserved its role in engineering design by means of its excellent mechanical properties and aesthetic appearance. Renewability and good strength-to-weight ratio render it a competitive alternative, further supported by scientific progress in wood research enabling more accurate and efficient design.

Wood, however, poses various challenges for engineers and researchers. Natural characteristics are different between species and may vary even within the same species, restricting the applicability of the results obtained from test specimens. The material properties cannot be engineered as opposed to artificial materials. Due to its complex inhomogeneous microstructure, wood is essentially an orthotropic material, and therefore the analytical approach to the fundamental mechanical behavior is limited. The study of its mechanical behavior is further complicated by the presence of natural features like knots, splits and grain slope deviations.

Parallel to grain, wood is customarily considered linear elastic and brittle in tension. In contrast, nonlinear material behavior of some kind is used in compression in the vast majority of studies; see, e.g., numerical analyses in [1–4]. For the description of stress-strain relationship beyond the elastic limit, one may consider several variants, such as completely plastic (e.g., [5, 6]), bilinear (e.g., [7–9]), higher-order (e.g., [10]), and even tri-linear [11]. Hill also suggested a bilinear anisotropic stress-strain relationship that may be used to predict orthotropic linear elastic–quasi-rigid behavior in tension and orthotropic linear elastic–perfectly plastic or bilinear behavior in compression; this model is applied in several studies, e.g., [12–15].

The numerical modelling of timber is mainly based on the finite element method. It is practically inescapable in modelling complicated setups such as the above-mentioned cases of knots or fiber deviations. In order to successfully quantify the real influence of knots on the structural performance of timber, computational models have to be fine-tuned to precisely recreate the three-dimensional state of stresses.

Knots and related grain deviations are considered the primary natural defects, and they have a negative impact on

Cite this article as: Saad, K., Lengyel, A. "A Parametric Investigation of the Influence of Knots on the Flexural Behavior of Timber Beams", Periodica Polytechnica Civil Engineering, 67(1), pp. 261–271, 2023. https://doi.org/10.3311/PPci.21360

the stiffness and overall capacity of timber elements [16]. The knot-related fiber deviations cause a local stress concentration, leading to an early tensile failure and ineffective compression capabilities [17]. The strength grading of timber structural elements would be more efficient if the influence of such defects were well known. The most affected properties are longitudinal tensile strength, modulus of rupture (MOR), compressive strength parallel to the grain, and modulus of elasticity (MOE). Knots often cause stress discontinuities in their vicinity and a deviation of the surrounding fibers in the tangential and radial planes.

Different non-destructive methods can be applied to measure the fiber deviation, e.g., X-ray technique [18], the CT-direction process (Computer Tomography) [19], laser confocal microscope [20], and the application of the tracheid effect scanning [21].

Live knots, which are organic parts of the wood material, are distinguished from dead knots, which are mechanically separated from the enclosing material. In terms of modelling, cases of rigid or elastic solids, as well as openings (voids), can be considered.

Numerical analysis was presented to evaluate the stress concentration due to knots approximated as openings. According to the findings, the normal stress distribution is sensitive to the distance between the knot's center, the extreme compression fiber of the timber beam, its diameter, and the amount of loads [22]. When knots were approximated by openings as opposed to solids, there were no significant differences in flexural strength, elastic modulus (MOE), or deflection [23]. Another investigation was carried out in which a two-dimensional numerical model was constructed and calibrated using four-point bending to investigate the influence of holes on timber beams' ultimate flexural capacities [24].

Knots can alternatively be represented by a cone or cylinder with a dive angle in the (LT) plane [25, 26]. For *Pinus sylvestris* L, the location of the rupture in relation to the position and size of knots and grain deviations was numerically predicted. Four-point bending and 2D numerical investigation were performed to test timber beams with knots approximated by openings and solids located throughout the beam height; however, the grain deviations around the knot were not smoothly constructed [27].

The stiffness and strength of wood components are mainly affected by associated knot fiber deviations. Localized fiber deviations cause extreme stress concentrations when the knot is situated in the tension side of a wood structural element under bending; however, stress concentrations are not significant for knots in the mid-cross-section [28]. The impact of knots and associated fiber deviations on the modulus of elasticity variations were investigated numerically by [29]. Other similar studies were also presented [30, 31]. A two-dimensional parametric finite element model was evaluated to investigate the influence of the size and position of knots on the behavior of structural timber members; knots were approximated by both openings and cylinders. However, these models cannot consider the effect of the diving angles and knot position along the beam longitudinal axis; the live-knot-model best replicates the actual behavior for knots on the compression side; nevertheless, the opening model proved most reliable for knots on the tension side. Beam bending strength decreased as knot size increased when the knot was located in the tension zone of the beam [32].

Moreover, the effect of size, position, and diving angle of different types of knots also located along the beam height, represented by elliptical oblique and rotated cones, on the bending strength of wood was parametrically investigated. It was found that the inclination has a beneficial impact on face knots when compared to similar perpendicular face knots since an inclined knot has a larger net cross-section [33]. Yet, the diving angle should be considered in two different directions, both up and down; therefore, it sometimes has a negative impact on the ultimate flexural capacity of the timber member. Furthermore, the effect of knot size and timber density on bending strength and stiffness was analyzed. It was found that changes in density and knot size substantially impact mechanical stress grades [34].

This study presents a parametric finite element analysis on the influence of size, position, and diving angle of conical knots and their associated grain deviations on the bending strength of *Picea abies* (Norway spruce) timber beams. Four-point bending tests were used to validate the three-dimensional finite element models. A number of independent studies in the literature were also processed to provide additional verification of the model used in this study. According to the techniques and findings, the three-dimensional numerical model may be regarded as a model for the complete structural element at a macro-scale that can accurately replicate the behavior of the entire defected timber element instead of just examining the impacts of knots. As a result, this output is intended to provide a better understanding of the natural heterogeneity and anisotropy of wood, enabling more effective use of the material.

2 Methodology

2.1 Timber beam properties considered for numerical simulation

The parametric finite element study presented here to investigate the effect of the characteristics of a conical knot on the flexural behavior of timber beams involved five parameters:

1. position of the knot along the beam longitudinal axis (X-axis),
2. position of the knot along the beam height (Y-axis),
3. knot radius,
4. knot diving angle (inclination), and
5. knot length.

The parametric investigation was carried out by combining the mathematical programming software MATLAB with the general-purpose finite element software ANSYS APDL to offer the user comprehensive and convenient control over the parametric simulations. The coupling is entirely automatic and does not require user intervention until the results are found and extracted.

A considerable number of characteristics are required for a comprehensive description of the wood material. The material properties applied for this specific study were adopted based on the literature. For a complete description, see [35].

2.2 Numerical modelling

The numerical simulations were performed with the help of the general-purpose finite element modelling package ANSYS. The linear elastic orthotropic material model was considered with unlimited capacity in tension, whereas it was combined with perfect plasticity beyond the linear range in compression; this can be represented by the Hill potential material model incorporated in the software. A bilinear anisotropic stress-strain relationship is used to enable the individual components of tension and compression yield stresses. The plastic or yield surfaces corresponding to the Hill model have an anisotropic work-hardening and associated flow rules.

The four-point bending setup was numerically reproduced by constraining the nodes located at a distance of 50 mm from both ends (i.e., at the supports) against vertical (Y) and horizontal transverse (Z) movements. Furthermore, one node located at the top at the mid-span of the beam was constrained against horizontal longitudinal (X) movement to avoid the rigid body motion. Displacement-controlled loading was applied at 350 mm, and 650 mm of the beam with a magnitude gradually increased up to 25 mm for all beams. It is recommended to use the 8-node solid element SOLID45 with a reduced integration since it is compatible with the anisotropic Hill material model. A 5 mm uniform meshing was assigned to the clear wood, the knot, and its surroundings. The knot was represented by the same solid element type. Common nodes were merged, and no contact elements were introduced.

Knots have a distinctive fiber pattern that differs from that of clear wood. The orthotropic directions of clear wood often do not apply for knots because of the irregularity and complexity of fiber distribution inside. Therefore, the behavior is approximated as isotropic. The material characteristics of the knot (modulus of elasticity and Poisson's ratio) were considered the same as the transverse direction material properties of the timber beam. The fiber arrangement in the knot and the clear timber are shown on a microscopic scale in Fig. 1.

The numerical model could parametrically generate knots and corresponding fiber deviations and assess and predict load-deflection curves of solid wood beams subjected to four-point bending. Fig. 2 illustrates the loading and boundary conditions of the numerical model.

For the generation of the knot geometry, a procedure introduced by the authors in a previous study [35] was employed. It is based on cutting up the specimens along vertical longitudinal planes, measuring and digitizing the fiber pattern around the knot in each slice to enable the creation of its three-dimensional numerical counterpart.

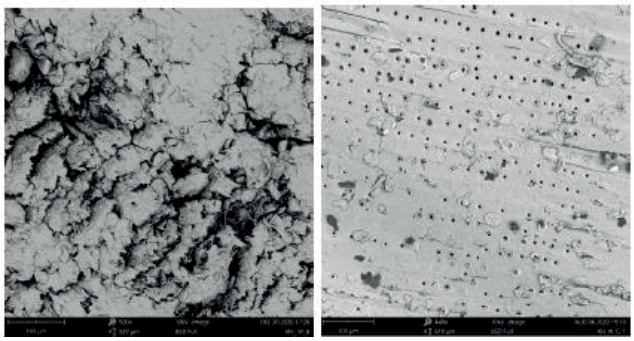

(a) (b)

Fig. 1 Microscopic fiber patterns: (a) knot fiber distribution, scope (horizontal) is 538 μm, (b) clear wood fiber distribution, scope (horizontal) is 610 μm

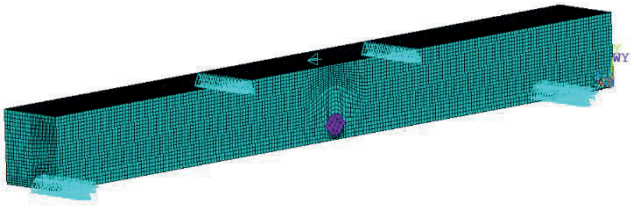

Fig. 2 Three-dimensional FE model

The generated fiber paradigm is also confirmed by visual inspection. The technique is illustrated in Fig. 3 via one of the test specimens analyzed in this study. (The experimental program is detailed in the next subsection.)

In this parametric study, all knots have a conical shape defined by several parameters. With the geometry of the knot given by the user, such as diameter, length, diving angles, and positions, the fiber paradigm in the disturbed zone is generated in each ply for the ANSYS simulations. As the fibers define the local principal axes of the orthotropic material, the material coordinate system in each finite solid element must be reoriented to follow the natural fiber deviation induced by the knot in its vicinity. Fig. 4 also shows a numerical model for one of the studied cases. Fig. 5 illustrates the material coordinate system orientations for one of the investigated studies.

2.3 Experimental procedures and validation of the numerical model

Two approaches are introduced for the validation of the finite element model: (1) experimental analysis performed by the authors and (2) FE and experimental studies performed by other authors.

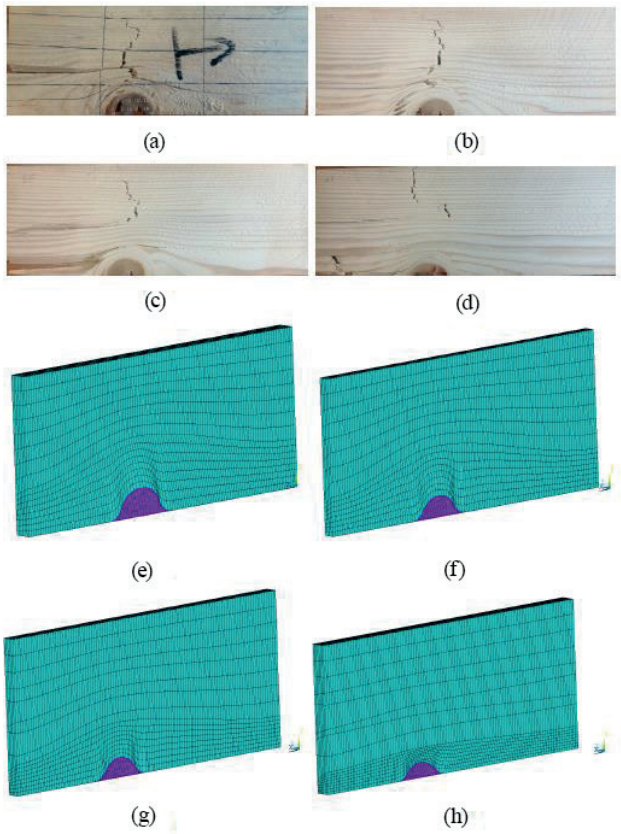

Fig. 3 Beam specimen (S3) containing a knot: (a)–(d) plies of the test specimen, and (e)–(h) the respective finite element mesh

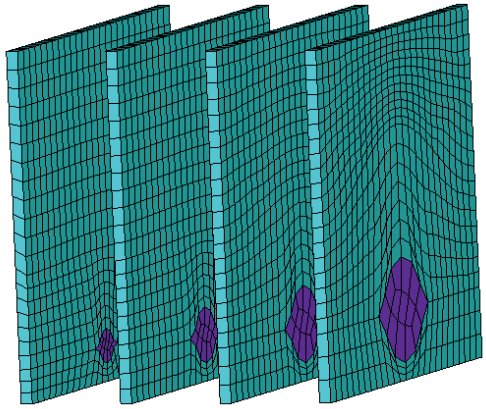

Fig. 4 Three-dimensional fiber paradigm in numerically generated slices across the beam thickness

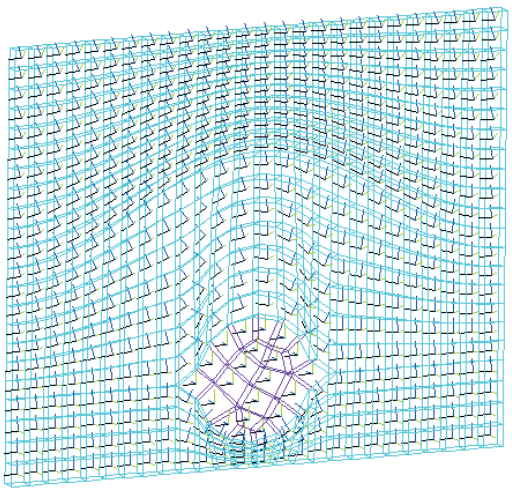

Fig. 5 Material coordinate system orientation in the finite element model in the vicinity of a knot

In the first approach experiments performed by the current authors was used. The author's experimental study was evaluated on six timber beams for the validation of the computational model [35]; see Table 1. The tested beams were sawn from Norway spruce wood. The simply supported specimens had a 900 mm clear span and a cross-section of 100 mm × 100 mm subjected to four-point bending delivered through a hydraulic jack in the center of the beam, allowing the beams to bend under continually increasing load. A load bridge was employed to transmit force at one and two-thirds of the span to accomplish four-point bending. A displacement-controlled force at a 3.5 mm/min rate was applied until the beam failed. The vertical movement of the loading device's head was adequately monitored and recorded. Experimental results proved that knots have a considerable impact on timber strengths. The existence of knots influences the global and local fiber orientation, which affects the mechanical behavior of the timber element.

Table 1 Specimen specifications (bending test). Columns refer to the specimen ID, presence of knot, ultimate mid-span deflection and force, respectively

Specimen	Knot	Disp. (mm)	Load (kN)
S1	N	34.03	67.24
S2	N	35.65	70.01
S3	Y	21.70	51.06
S4	Y	18.22	42.82
S5	Y	20.80	50.68
S6	Y	23.88	43.23

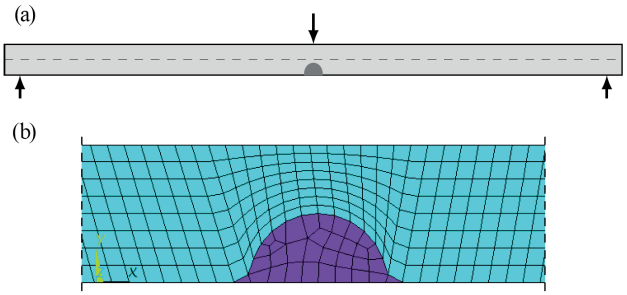

Fig. 6 Case study 1 for the validation of the model using Ref. [23] (a) test beam, (b) constructed FE mesh

The load-deflection curves obtained in the four-point bending tests [35] serve as a basis for the validation of the numerical model. The model considers linearly elastic and perfectly plastic behavior in compression and unlimited tension capacity, assuming no plasticity in tension. The numerically generated curves obtained by applying the Hill anisotropic material model are displayed against the measured load-deflection curves, and the endpoint of the curve corresponds to the actual tensile strength.

Furthermore, tensile failure was experienced in the surroundings of the knot, resulting in a considerable decrease in ultimate capacity: approx. 28% for a particular case (S3) where the knot had an apparent diameter of 35 mm, 36 mm of length, and essentially no diving angles. It was situated at the mid-span of the beam, in the extreme tension zone. It can be interpreted such that the early tension failure occurred due to the local fiber deviation around the knot, and the load-deflection curve displayed moderate non-linearity.

The second approach is based on a few previously published independent studies where experimental and numerical investigations were carried out regarding the effects of knots on timber behavior. In one study, the authors investigated the mechanical similarities between knots and openings through an experimental analysis [23]. Fig. 6 shows the sketch of the test arrangement for one of the investigated beams containing a cylindrical knot, as well as our reproduction of the three-dimensional finite element mesh in the vicinity of the knot. The numerical model could produce the same experimental load-deflection response using the specified wood properties and dimensions (see Fig. 6). Force load at 12 mm displacement in the experiment and the simulation was 400 kN and 396 kN, respectively.

In another paper, a parametric finite element study was introduced to investigate the effect of knot size and position on the modulus of rupture (MOR) of timber using the ANSYS APDL language [33]. The authors applied the Tsai-Wu failure criterion to determine the failure initiation. The knot in this case study was cylindrical with a diameter of one-sixth of cross-section height located at the mid-span of the beam at different vertical positions (one-eighth and two-eighths of the height from the bottom). It was found that the MOR increased by 75.6% when the knot was moved from the former position to the latter. In the present work, the beams were remodeled using our technique and the material properties provided by the referenced paper, yielding an increase of 73% in MOR, almost identical to the reference.

In the third study [27], the authors conducted experiments on beam specimens and respective finite element simulations to determine the ultimate load. The Tsai-Wu failure criterion was used in the numerical calculations to catch the failure initiation. In one of the investigated cases, the ultimate load of 7.9 kN and 8.4 kN was obtained in the test and the simulation, respectively. The schematic representation of the test arrangement, the finite element mesh and the Tsai–Wu contour plot at failure are shown in Figs. 7(a), (b) and (c), respectively. In the present work, the model of the test specimen is reconstructed, yielding an ultimate load of 8.2 kN. The mesh and the Tsai-Wu plot in the vicinity of the knot are shown in Fig. 7(d) and (e), respectively. The technique applied in the present work both provided a more realistic mesh and a more accurate approximation of the test results than in the referenced paper.

3 Results and discussion

3.1 Load-displacement curves and failure prediction

The load-deflection curves produced by the authors' own experimental program were used to validate the numerical models. The simulated load-deflection curves in both linear and nonlinear ranges closely resemble those found in the experiments.

Non-linearity is only considered under compression because timber cannot become ductile in tension. Compression ductility is thoroughly utilized in the

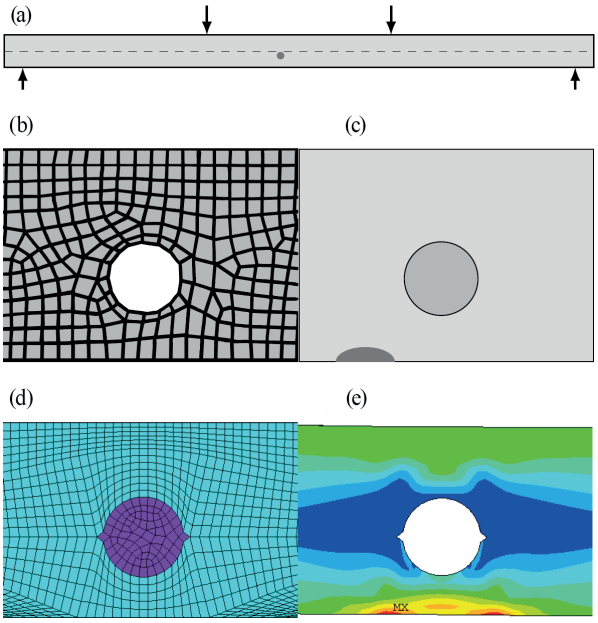

Fig. 7 Case study 3 for the validation of the model using Ref. [27] (a) test arrangement, (b) sketch of the FE mesh around a knot applied in the reference, (c) sketch of the respective Tsai–Wu contour plot indicating the failure spot, (d) FE mesh applied in the present work, (e) respective Tsai–Wu plot

knot-free specimens, which indicates the nonlinear component of the load-displacement curves. However, knots cause local fiber waviness, significantly impacting the beam's ultimate flexural capacity. The effect of fiber deviations is determined by the knot's location, length, diameter, and diving angles.

The experiments revealed that the tensile failure was confined to the knot vicinity causing ultimate tensile failure with a significant loss in the maximum flexural capacity, emphasizing the significance of knot-induced local fiber waviness. The premature tension rupture caused by the local fiber deviation due to the presence of the knot causes the load-deflection curve to undergo moderate non-linearity. This type of failure prevents the full utilization of the compression capacity of the wood, resulting in insufficient ductility.

Local grain deviation generates stress concentrations (normal and shear) around the knot, yielding localized failure followed by total beam damage, especially for knots found in the tension zone. A suggested failure criterion was proposed by [36] for analyzing the failure in anisotropic materials that take orthotropy and interaction influences into consideration and different strengths in tension and compression. For failure evaluations, the Tsai–Wu failure criterion is introduced as $F_i\sigma_i + F_{ij}\sigma_i\sigma_j = 1$, where σ_i are the stresses in Voigt notation (i = 1,…, 6) and F_i and F_{ij} are experimentally determined strength parameters. Failure occurs when the expression reaches or exceeds unity. The unit value of the TWSR of ANSYS (the inverse of the Tsai–Wu failure index) indicates initial failure; however, the TWSR index should be interpreted as a damage initiation index as it provides details about the specimen's damage initiation [37]. The maximum permissible material strength values (stress or strain) must be defined for the damage initiation criteria. The material is considered to be homogenous, and the ultimate permissible strength for every finite element is equivalent. This task aims to identify the qualitative and quantitative failure patterns expected by Tsai–Wu. The pattern indicates that failure initiation takes place near the knot. After identifying the initial deterioration, damage progression rules may be used to track material degradation in a detailed configuration [38]. Experiment findings verified that the failure was localized to the deviated fiber zone without causing damage to the knot itself.

3.2 The effect of the position of the knot along the beam's longitudinal axis

The loss of ductility highlights an essential distinction between timber beams with and without knots. At the same stress level, the presence of the knot induces early tensile failure in the wood, and as a result, a lower ultimate load can only be reached.

In this parametric study, the knot has a conical shape with a length of 50 mm, a visible diameter of 30 mm, diving angles of zero degrees, the distance from the edge of the knot to the extreme tension fiber is 5 mm, and the longitudinal position is set to be multiples of 50 mm, see Fig. 8. Table 2 presents the obtained maximum capacities of the timber beams in terms of the knot position.

Results showed that the effects of the knot on flexural behavior are minor when it is found near the support. A recognizable drop in ultimate capacity of 10.42% was achieved when the knot was located at 25% of the beam's entire length. However, when the knot was situated in the beam mid-span, the loss of load-bearing capacity reached

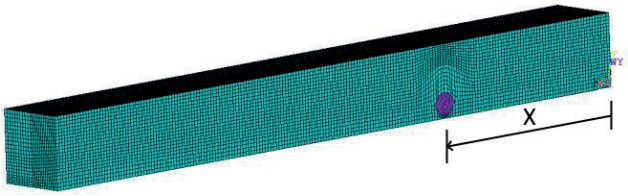

Fig. 8 Positioning the knot along the beam longitudinal axis (X = 300 mm)

Table 2 Capacity vs knot position along the longitudinal axis X

Position X (mm)	Capacity (kN)	Position X (mm)	Capacity (kN)
No knot	82.415	500	50.452
100	81.400	550	50.430
150	80.530	600	50.284
200	80.390	650	54.690
250	73.901	700	61.951
300	61.951	750	73.901
350	54.691	800	80.390
400	50.284	850	80.530
450	50.430	900	81.400

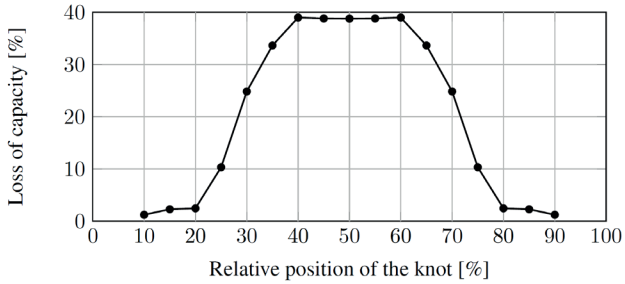

Fig. 9 Loss of capacity versus relative position of the knot along the beam longitudinal axis

39%, as illustrated in Fig. 9. The longitudinal position also affects the failure mode. When the knot is close to the support, a typical tension failure at mid-span develops (Fig. 10(a)), while if it is located in a high bending moment zone (i.e., near mid-span), the failure is initiated in the vicinity of the knot in the disturbed fiber zone (Fig. 10(b)).

3.3 The effect of the position of the knot along the beam height

In this section, the knot has a fixed diameter of 30 mm, diving angles of 0 degrees, and a length of 50 mm, and it is located in the middle of the beam span. The parametric vertical position Y is given by the lowermost point of the knot from the bottom edge of the beam, see Fig. 11. Table 3 presents the obtained numerical values of the maximum capacities for each beam configuration.

The Tsai–Wu failure criterion reveals different stress behavior and failure mechanism for different knot positions. If the knot is located in the tension zone, the cross-section area effective for tension is significantly reduced, and the stress state is disturbed due to fiber deviations leading to early failure. In this study, the maximum loss of capacity reached 69% for the lowermost position of the knot. However, if the knot is located in the compression zone,

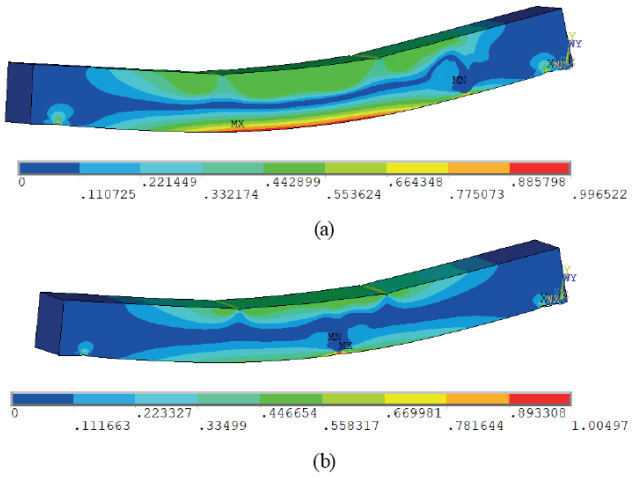

Fig. 10 The inverse of the Tsai–Wu failure index (a) typical tension failure - (b) failure due to the knot

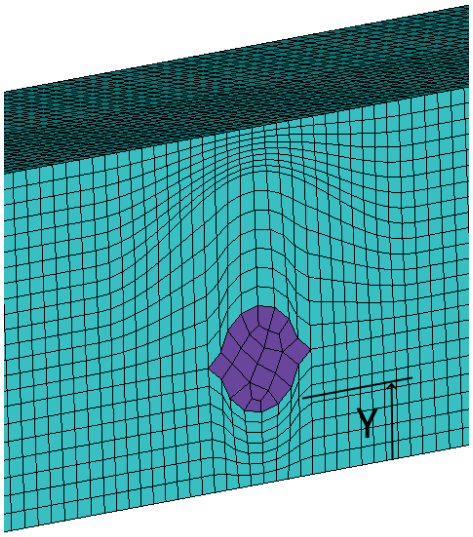

Fig. 11 Positioning the knot throughout the beam height

Table 3 Capacity vs knot position (Y axis)

Position Y (mm)	Capacity (kN)
0	25.412
5	50.438
10	61.957
15	65.212
20	65.212
25	70.803
30	73.251
65	77.730

the load-bearing capacity is only marginally affected, and elastic-plastic compression stresses are more effectively utilized, leading to both higher capacity and ductility of the beam. Capacity versus vertical position is shown in Fig. 12.

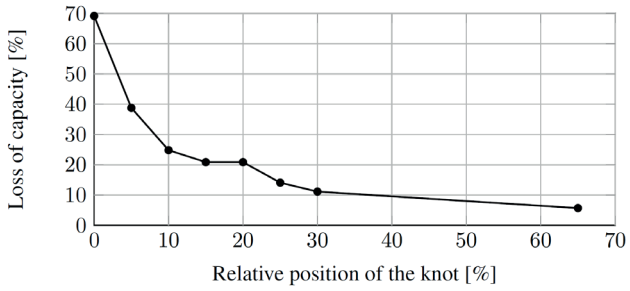

Fig. 12 Loss of capacity versus relative position of the knot throughout the beam height measured from the bottom

3.4 Effect of knot radius

Fiber deviation is mainly affected by the size of the knot. The larger the knot, the more significant disturbance it creates in the fiber paradigm. The knot in this investigation has a 50 mm constant length, 0 degrees for vertical and horizontal diving angles, and is situated at the beam mid-span. The only parameter in this study is the knot radius; see Fig. 13.

Table 4 and Fig. 14 clearly show a significant reduction of the ultimate capacity of almost 40% when the knot has a radius of 20 mm (40% of the whole cross-section).

3.5 The effect of the knot diving angle

In this section, the diving angle of the knot (the vertical inclination) was considered. The knot is considered conical with an apparent diameter of 30 mm (30% of the beam height), located in the mid-span of the beam and at a distance of 5 mm from the extreme tension fibers with variable dive angle. The variation in the fiber orientations in the LT plane is generated automatically. Fig. 15 shows examples of a negative diving angle (inclination upward) and a positive one (downward).

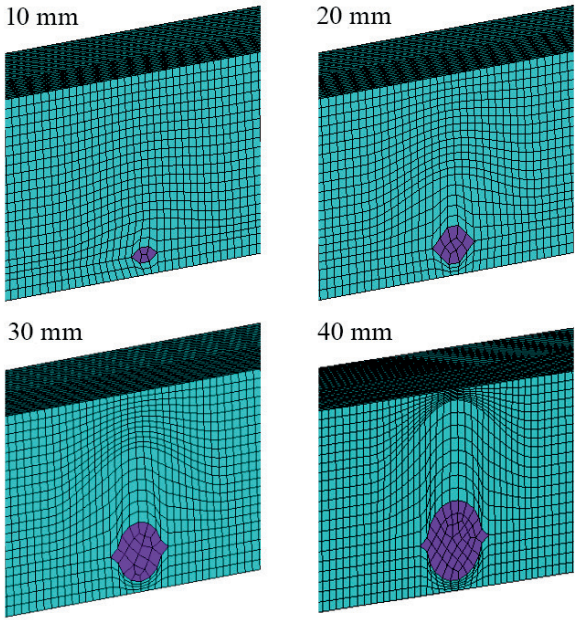

Fig. 13 Finite element mesh for various knot radii

Table 4 Capacity vs knot radius

Knot radius (mm)	Capacity (kN)
0	82.415
5	69.024
10	62.523
15	50.452
20	49.552

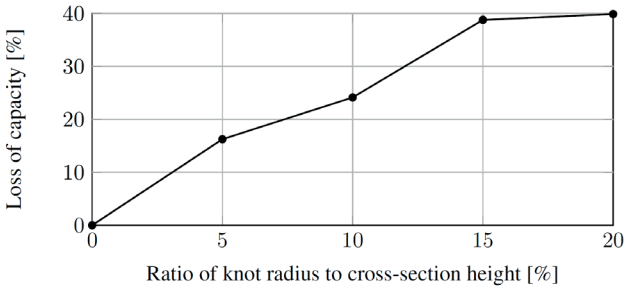

Fig. 14 Loss of capacity versus knot radius

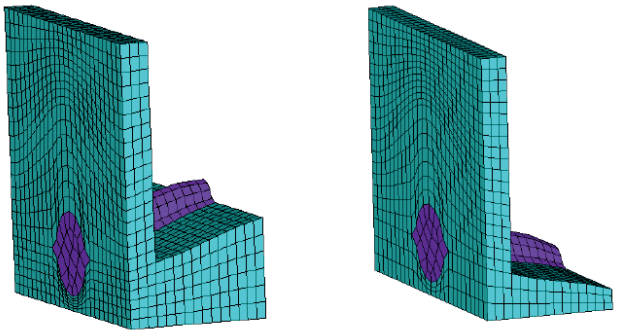

Fig. 15 Mesh of the knot and its vicinity at (a) –25 degrees diving angle, (b) +5 degrees diving angle

Table 5 and Fig. 16 show the load-bearing capacity in terms of the diving angle. It is observed that the negative diving angle (Fig. 15(a)) increases the part of the cross-section area under the knot in the tension zone where the brittle failure usually occurs, resulting in an enhancement in the ultimate capacity (by up to 25% in this study) in comparison to the zero diving angle. However, a positive diving angle has an opposite effect (Fig. 15(b)), as it reduces the net cross-section in the tension zone and causes a drop in the ultimate capacity.

3.6 The effect of the knot length

In the last parametric study, the length of the knot varied between zero (no knot) to the full cross-section width. The knot was located at the mid-span of the beam at a distance

Table 5 Capacity vs knot diving angle

Vertical diving angle (degree)	Capacity (kN)
5	36.005
0	50.452
-5	50.479
-10	54.647
-20	58.511
-25	58.437
-30	58.479
-35	58.441
-40	61.811

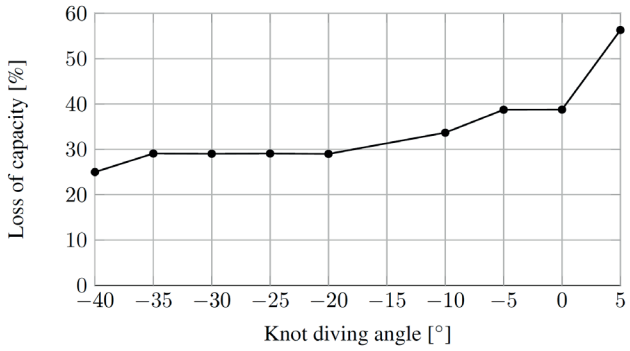

Fig. 16 Loss of capacity versus knot diving angle

Table 6 Capacity vs knot length

Length (mm)	Capacity (kN)
0	82.415
10	69.558
20	59.009
30	53.404
40	50.932
50	50.273
60	46.185
70	42.822
80	38.174
100	36.839

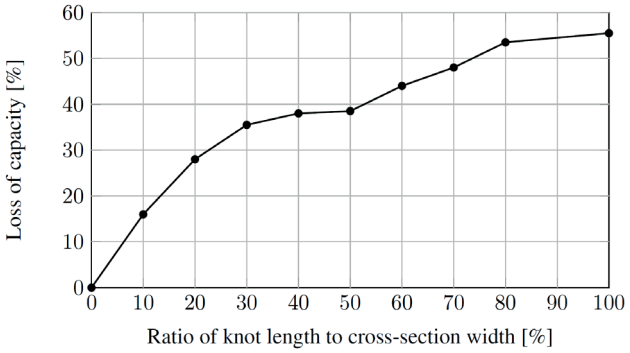

Fig. 17 Loss of capacity versus knot length

of 5 mm from the bottom edge of the beam in the tension zone. It was found that the failure was localized and confined to the knot vicinity in all the cases.

Table 6 and Fig. 17 show the capacity of the beam in terms of the knot length along the cross-section width. It is observed that the capacity rapidly drops initially when the length increases, indicating that even a short knot can be detrimental to the mechanical behavior due to the stress disturbance it creates. A full-length knot leads to a loss of 55% in this study.

4 Conclusions

A numerical technique was developed to recreate the fully three-dimensional finite element model of the vicinity of the knot parametrically in terms of the user-defined geometric properties of the knot.

The parametric investigation was presented in this study to numerically evaluate the impact of knots in timber beams on the flexural load-bearing capacity with the help of the finite element method. This comprehensive parametric study involved all significant geometric properties such as knot size (diameter and length), location (both longitudinally and vertically), and the diving angle. The three-dimensional fiber paradigm was parametrically generated in the finite element models based on a technique provided by the authors, which could accurately produce the three-dimensional fiber deviations induced in the knot vicinity.

The model was partly validated by the authors' own experimental program involving Norway spruce beams subjected to four-point bending tests and partly by numerical and experimental data available in the literature from independent research studies. The model validation resulted in a good agreement between the experimental and simulated load-deflection curves and failure predictions for the tested specimens in bending. The general observation regarding the numerical and experimental investigations presented here is that knots located in the tension zone cause an early tension failure attributed to considerable fiber inclination around the knot and, therefore, the ineffective utilization of fiber strength. This, in turn, results in unsatisfactory compression capacity utilization as well. The main findings of the parametric simulations are summarized as follows:

1. Knots located in the tension zone in high bending moment sections (mid-span) cause the largest loss capacity (39%); however, other locations also have a negative effect due to the extent of the disturbed

fiber paradigm around the knot. Horizontal position has a negative effect even if not in the maximum bending moment zone.
2. Knots located in the compression zone have considerably less effect on capacity as well as ductility.
3. Lower capacity was obtained for bigger knot radii since they induced large fiber deviations.
4. A diving angle with an upward inclination positively affects the load-bearing capacity, whereas a downward inclination acts contrary by reducing the net cross-section available for tension.
5. Loss of capacity monotonously increases with knot length, and the most rapid change is observed for short knots, indicating that even a short knot can be critical to mechanical behavior.

It is also important to note that tensile failure in wood is typically initiated in the wood material around the knot and not in the knot itself; therefore, accurate modelling of the knot vicinity in terms of the geometry of the fiber paradigm and the associated material law is of the highest importance in order to obtain adequate predictions on the mechanical behavior.

Acknowledgements

The presented work was conducted with the financial support of the K138615 project of the Hungarian National Research, Development, and Innovation Office. The authors wish to thank Dr. Nehme Salem Georges and the Department of Construction Materials and Technologies for their full support in conducting the experiments.

References

[1] Raftery, G. M., Harte, A. M. "Nonlinear numerical modelling of FRP reinforced glued laminated timber", Composites Part B: Engineering, 52, pp. 40–50, 2013. https://doi.org/10.1016/j.compositesb.2013.03.038

[2] Čizmar, D., Sørensen, J. D., Kirkegaard, P. H., Rajčić, V. "Robustness analysis of a timber structure with ductile behaviour in compression", [pdf] In: Proceedings of the Final Conference of COST Action TU0601: Robustness of Structures, Prague, Czech Republic, 2011, pp. 17–32. Available at: https://vbn.aau.dk/ws/files/53021053/Robustness_Analysis_of_a_Timber_Structure_with_Ductile_Behaviour_in_Compression.pdf

[3] Gilfillan, J. R., Gilbert, S. G., Patrick, G. R. H. "The use of FRP composites in enhancing the structural behavior of timber beams", Journal of Reinforced Plastics and Composites, 22(15), pp. 1373–1388, 2003. https://doi.org/10.1177/073168403035583

[4] Buchanan, A. H. "Bending strength of lumber", Journal of Structural Engineering, 116(5), pp. 1213–1229, 1990. https://doi.org/10.1061/(ASCE)0733-9445(1990)116:5(1213)

[5] Nowak, T. P., Jasieńko, J., Czepiżak, D. "Experimental tests and numerical analysis of historic bent timber elements reinforced with CFRP strips", Construction and Building Materials, 40, pp. 197–206, 2013. https://doi.org/10.1016/j.conbuildmat.2012.09.106

[6] Nadir, Y., Nagarajan, P., Ameen, M., Arif, M. M. "Flexural stiffness and strength enhancement of horizontally glued laminated wood beams with GFRP and CFRP composite sheets", Construction and Building Materials, 112, pp. 547–555, 2016. https://doi.org/10.1016/j.conbuildmat.2016.02.133

[7] Fiorelli, J., Dias, A. A. "Glulam beams reinforced with FRP externally-bonded: theoretical and experimental evaluation", Materials and Structures, 44, pp. 1431–1440, 2011. https://doi.org/10.1617/s11527-011-9708-y

[8] Johnsson, H., Blanksvärd, T., Carolin, A. "Glulam members strengthened by carbon fibre reinforcement", Materials and Structures, 40, pp. 47–56, 2007. https://doi.org/10.1617/s11527-006-9119-7

[9] Schober, K.-U., Harte, A. M., Kliger, R., Jockwer, R., Xu, Q., Chen, J.-F. "FRP reinforcement of timber structures", Construction and Building Materials, 97, pp. 106–118, 2015. https://doi.org/10.1016/j.conbuildmat.2015.06.020

[10] Li, Y.-F., Tsai, M.-J., Wei, T.-F., Wang, W.-C. "A study on wood beams strengthened by FRP composite materials", Construction and Building Materials, 62, pp. 118–125, 2014. https://doi.org/10.1016/j.conbuildmat.2014.03.036

[11] Moses, D. M., Prion, H. G. I. "Anisotropic plasticity and failure prediction in wood composites", 2002. [online] Available at: https://ansys-net.svsfem.cz/?mycat=search&mytype=Natural&mystring=Anisotropic+plasticity+and+failure+prediction+in+wood+composites&submit=Search

[12] Madenci, E., Guven, I. "The Finite Element Method and Applications in Engineering Using ANSYS®", Springer, 2015. ISBN 978-1-4899-7549-2 https://doi.org/10.1007/978-1-4899-7550-8

[13] Hill, R. "A theory of the yielding and plastic flow of anisotropic metals", Proceedings of the Royal Society A, Mathematical, Physical and Engineering Sciences, 193(1033), pp. 281–297, 1948. https://doi.org/10.1098/rspa.1948.0045

[14] Shih, C. F., Lee, D. "Further developments in anisotropic plasticity", Journal of Engineering Materials and Technology, 100(3), pp. 294–302, 1978. https://doi.org/10.1115/1.3443493

[15] Valliappan, S., Boonlaulohr, P., Lee, I. K. "Nonlinear analysis for anisotropic materials", International Journal for Numerical Methods in Engineering, 10(3), pp. 597–606, 1976. https://doi.org/10.1002/nme.1620100309

[16] Senalik, C. A., Farber, B. "Mechanical properties of wood", In: Wood handbook: Wood as an engineering material", USDA Forest Service, Forest Products Laboratory, Madison, WI, USA, Rep. FPL-GTR-282, 2010. [online] Available at: https://www.fs.usda.gov/treesearch/pubs/62200

[17] Foley, C. "Modeling the effects of knots in structural timber", PhD Thesis, Lund University, 2003. https://doi.org/10.13140/RG.2.2.30965.22243

[18] Cramer, S., Shi, Y., McDonald, K. "Fracture modeling of lumber containing multiple knots", [pdf] In: Proceedings of the International Wood Engineering Conference 1996, New Orleans, LA, USA, 1996, pp. 288–294. Available at: https://www.fpl.fs.usda.gov/documnts/pdf1996/crame96b.pdf

[19] Ekevad, M. "Method to compute fiber directions in wood from computed tomography images", Journal of Wood Science, 50, pp. 41–46, 2004. https://doi.org/10.1007/s10086-003-0524-z

[20] Mihashi, H., Navi, P., Sunderland, H., Itagaki, N., Ninomiya, S. "Micromechanics of knot's influence on tensile strength of Japanese cedar", In: 1st RILEM Symposium on Timber Engineering, Stockholm, Sweden, 1999, pp. 181–190. ISBN: 2912143101

[21] Briggert, A., Hu, M., Olsson, A., Oscarsson, J. "Tracheid effect scanning and evaluation of in-plane and out-of-plane fiber direction in Norway spruce timber", Wood and Fiber Science, 50(4), pp. 411–429, 2018. https://doi.org/10.22382/wfs-2018-053

[22] Burawska, I., Tomusiak, A., Turski, M., Beer, P. "Local concentration of stresses as a result of the notch in different positions to the bottom surface of bending solid timber beam based on numerical analysis in Solidworks Simulation environment", Annals of Warsaw University of Life Sciences - SGGW, Forestry and Wood Technology 73, pp. 192–198, 2011.

[23] Burawska, I., Zbiec, M., Kalicinski, J., Beer, P. "Technical simulation of knots in structural wood", Annals of Warsaw University of Life Sciences – SGGW, Forestry and Wood Technology. 82, pp. 105–112, 2013.

[24] Williams, J. M., Fridley, K. J., Cofer, W. F., Falk, R. H. "Failure modeling of sawn lumber with a fastener hole", Finite elements in Analysis and Design, 36(1), pp. 83–98, 2000. https://doi.org/10.1016/s0168-874x(00)00010-x

[25] Kandler, G., Lukacevic, M., Füssl, J. "An algorithm for the geometric reconstruction of knots within timber boards based on fibre angle measurements", Construction and Building Materials, 124, pp. 945–960, 2016. https://doi.org/10.1016/j.conbuildmat.2016.08.001

[26] Guindos, P., Guaita, M. "A three-dimensional wood material model to simulate the behavior of wood with any type of knot at the macro-scale", Wood Science and Technology, 47, pp. 585–599, 2013. https://doi.org/10.1007/s00226-012-0517-4

[27] Baño, V., Arriaga, F., Soilán, A., Guaita, M. "Prediction of bending load capacity of timber beams using a finite element method simulation of knots and grain deviation", Biosystems Engineering, 109(4), pp. 241–249, 2011. https://doi.org/10.1016/j.biosystemseng.2011.05.008

[28] Cramer, S. M., Goodman, J. R. "Model for stress analysis and strength prediction of lumber", Wood and Fiber Science, 15(4), pp. 338–349, 1983.

[29] Hu, M. "Studies of the fibre direction and local bending stiffness of Norway spruce timber: for application on machine strength grading", PhD Thesis, Linnaeus University, 2018.

[30] Foley, C. "A three-dimensional paradigm of fiber orientation in timber", Wood Science and Technology, 35, pp. 453–465, 2001. https://doi.org/10.1007/s002260100112

[31] Lukacevic, M., Kandler, G., Hu, M., Olsson, A., Füssl, J. "A 3D model for knots and related fiber deviations in sawn timber for prediction of mechanical properties of boards", Materials & Design, 166, 107617, 2019. https://doi.org/10.1016/j.matdes.2019.107617

[32] Baño, V., Arriaga, F., Guaita, M. "Determination of the influence of size and position of knots on load capacity and stress distribution in timber beams of pinus sylvestris using finite element model", Biosystems Engineering, 114(3), pp. 214–222, 2013. https://doi.org/10.1016/j.biosystemseng.2012.12.010

[33] Guindos, P., Guaita, M. "The analytical influence of all types of knots on bending", Wood Science and Technology, 48, pp. 533–552, 2014. https://doi.org/10.1007/s00226-014-0621-8

[34] Grant, D. J., Anton, A., Lind, P. "Bending strength, stiffness, and stress-grade of structural pinus radiata: effect of knots and timber density", New Zealand Journal of Forestry Science, 14(3), pp. 331–348, 1984.

[35] Saad, K., Lengyel, A. "Accurate finite element modelling of knots and related fibre deviations in structural timber", Journal of King Saud University - Engineering Sciences, in press. (Accepted for publication January 2022) https://doi.org/10.1016/j.jksues.2022.01.005

[36] Tsai, S. W., Wu, E. M. "A general theory of strength for anisotropic materials", Journal of Composite Materials, 5(1), pp. 58–80, 1971. https://doi.org/10.1177/002199837100500106

[37] Barbero, E. J., Shahbazi, M. "Determination of material properties for ANSYS progressive damage analysis of laminated composites", Composite Structures, 176, pp. 768–779, 2017. https://doi.org/10.1016/j.compstruct.2017.05.074

[38] Lemaitre, J., Desmorat, R. "Isotropic and anisotropic damage law evolution", In: Lemaitre, J. (ed.) Handbook of Materials Behavior Models, Vol II, Academic Press, 2001, pp. 513–524, 2001. ISBN 978-0-12-443341-0 https://doi.org/10.1016/B978-012443341-0/50057-0